# The study of a gravitational influence of a nearly passing star on the primordial Kuiper belt

**L. Neslušan and T. Paulech**

[1] *Astronomical Institute of the Slovak Academy of Sciences*
*059 60 Tatranská Lomnica, The Slovak Republic*

[2] *Astronomical Institute of the Slovak Academy of Sciences, Interplanetary*
*Matter Division, Dúbravská cesta 9, 845 04 Bratislava, The Slovak Republic*

**Abstract.** Through a numerical integration of the orbits of test particles representing small bodies in the outer region of a once existing proto-planetary disc, which were perturbed by a nearly passing star and Neptune, we answer the question on a possibility that the observed truncation of the Kuiper belt at 50 AU was caused just by a close encounter of the Solar System with a star. We consider a spectrum of possible encounter relative velocities, geometries, and masses of the perturbing star. Though the stellar perturbation tends to increase the number density of the classical Kuiper-belt objects (CKBOs) inside 50 AU in some cases, Neptune simultaneously reduces again this number density. The ratio of the discovery probabilities of CKBOs within 50 AU and beyond this distance appears to be comparable, for several combinations of the encounter parameters, to a critical ratio at which the truncation could be explained by a perturbative stellar passage. However, even these interesting combinations are not acceptable, because the simultaneous change of the velocity of the Sun turns out here to be so large that the Oort cloud would have been stripped and no dynamically new comets could be observed. In conclusion, no stellar encounter, with a relative velocity comparable or larger than about $5 \, \mathrm{km \, s^{-1}}$, could cause the truncation of the Kuiper belt after the epoch when the macroscopic bodies in the belt and a significant fraction of the Oort cloud were formed.

**Key words:** Kuiper belt – edge beyond 50 AU – stellar perturbations

## 1. Introduction

Foe about the last decade, several hundreds of small bodies have been discovered in the region of Neptune's orbit and beyond. It has been revealed that these bodies can be classified into three dynamical groups: "resonant population" containing bodies which are in a mean-motion resonance with Neptune, "classical Kuiper belt objects" (CKBOs) in low eccentric orbits inclined to the invariable plane of the planets, and the so-called "scattered disc" containing the bodies in eccentric and highly inclined orbits.

All trans-Neptunian objects (TNOs) are the remnant bodies of a once existing proto-planetary disc. According to the theoretical models of this disc, its outer part should still contain bodies in orbits with a very low eccentricity and inclination to the invariable plane. The number density of the objects should decrease monotonously with the increasing heliocentric distance. After knowing the orbits of several hundreds of TNOs, it is clear that their actual population differs from our original expectations. Only CKBOs resemble the original outer part of the proto-planetary disc, though the mean eccentricity and inclination are too high even for this group.

Another problem with the classical Kuiper belt is its abrupt outer edge at the heliocentric distance of $\approx 50\,\mathrm{AU}$ (Jewitt et al., 1998; Chiang and Brown, 1999; Allen et al., 2001; Gladman et al., 2001; Malhotra, 2001; Trujillo and Brown, 2001; Trujillo et al., 2001a, 2001b; Allen et al., 2002). Ida et al. (2000) and further authors (Kobayashi and Ida, 2001; Levison et al., 2004; Melita et al., 2005) suggested that this truncation of the belt was caused by a nearly passing star, which dispersed the orbits of the objects beyond the mentioned critical distance.

In this paper, we follow the idea that the truncation of the Kuiper belt was caused by a passing star and map a corresponding gravitational effect on small bodies in the outer part of the proto-planetary disc. In principle, a star could cause the truncation of the disc in two ways. First, it could excite the orbits of solid particles before their growth to the sizes large enough to be detectable within the present survey designed for the discoveries of new TNOs. The particles in the excited orbits could not, then, collide slowly, stick together and form larger objects (Kobayashi and Ida, 2001). Their mutual collisions became less frequent and destructive. Second, the material in the outer part of the proto-planetary disc accreted into the bodies large enough to be detected, but the star enlarged the eccentricities, semi-major axes, and inclinations of their orbits, therefore their number density considerably decreased in the concerned region (Ida et al., 2000; Levison et al., 2004; Melita et al., 2005).

In this work, we study the second possibility focussing ourselves mainly to a random stellar encounter, which could happen sometime during the age of the Solar System with a relatively high encounter velocity. The effect on the CKBOs is followed by a simulation of a strong stellar perturbation, the perturbation of the Neptune including, on a set of test particles (TPs) representing the bodies in an original, not depleted, outer part of the proto-planetary disc. Our simulation is improved in comparison with similar simulations of previous researchers (Levison et al., 2004; Melita et al., 2005) assuming a larger spectrum of stellar masses and orbital geometries of an encounter, and taking into account also the perturbation by the Neptune, which appears to be very important in the given context. In fact, we attempt to map the orbital phase space of the stellar approach and find the intervals of characteristics for which the suggested explanation of the outer edge is possible.

Levison et al. (2004) pointed out that the encounters characterized by some stellar masses and geometries could not happen after the formation of the Oort cometary cloud. Namely, a very strong stellar perturbation on the Sun would have changed the vector of solar velocity in the Galaxy much more than the velocity vectors of the comets in their distant reservoir. The Sun would have moved in a new trajectory through the Galaxy, while the bodies in the cometary cloud would have moved in their very-little-changed original trajectories. In this way, the cometary cloud would have been stripped. Therefore, when we consider the specific mass of the approaching star and its minimum heliocentric distance, we confront the situation with this constraint and decide whether the encounter could happen whenever during the period of the Solar-System existence or only during a short period before the formation of the Oort cloud.

## 2. Initial assumptions

In the beginning of our simulations, we assume a set of TPs in nearly circular and co-planar orbits in heliocentric distances corresponding to the outer part, beyond Neptune, of the proto-planetary disc. Specifically, we assume a grid of orbital elements with a randomly distributed eccentricity in the interval from 0 to 0.01, randomly distributed argument of perihelion ranging from 0 to $2\pi$ radians, and randomly distributed inclination to the mean plane of the set ranging from 0 to 0.01 radians. Further, we assume 12 discrete values of the longitude of ascending node, from 15° to 345° with the step of 30°. The heliocentric distance of the TPs, $r$, in the moment of crossing the ascending node varies from 35 AU to 100 AU with the step of 1 AU. Thus, we have the set of 792 TPs.

The initial orbit of Neptune is co-planar with the orbits of TPs. We attempt to consider a realistic initial orbit of this planet taking the same orbital elements as the orbit had in year 2000, specifically in the moment of JDT = 2451600.5 (Astronomical Almanac for year 2000), in each simulation.

In a given simulation, we assume a perturbing star with mass $M_*$ moving in the hyperbolic orbit with perihelion distance $q_*$ and encounter velocity with the Sun $v_\infty$ (the relative heliocentric velocity at infinity). For a given combination of $M_*$ and $q_*$, we consider three discrete values of $v_\infty$ equal to 5, 10, and 15 km s$^{-1}$, six discrete values of the inclination of stellar orbit, $i_*$, to the mean orbit of TPs, and six discrete values of the argument of perihelion of stellar orbit, $\omega_*$. Both $i_*$ and $\omega_*$ range from 15° to 165° with the step of 30°. Because of the axial symmetry, we consider only a half of the entire possible interval of $\omega_*$ values as well as a single value (zero) of the longitude of ascending node of each stellar orbit considered.

To find the most appropriate mass and geometry of the approach of a perturbing star to the Kuiper belt, we also modify the assumed values of the mass, $M_*$, and stellar perihelion, $q_*$. Specifically, we assume (a) a closer passage of a less massive star and (b) a more distant passage of a more massive star. In

case (a), $M_*$ ranges from 0.1 to 0.5 $M_\odot$ (solar masses) with the discrete step of 0.1 $M_\odot$ and $q_* = 70$, 100, and 200 AU, while in case (b) $M_*$ ranges from 0.25 to 1.25 $M_\odot$ with the discrete step of 0.25 $M_\odot$ and $q_* = 500$, 1000, and 1500 AU.

We follow the dynamical evolution of the perturbing star, Neptune, and set of the TPs through a numerical integration of their orbits using the simplectic RMVS3 integrator from the SWIFT package (Levison & Duncan, 1994). In the beginning of the integration, the star is situated in the pre-perihelion arc of its orbit in the heliocentric distance of 10 000 AU or 20 000 AU in case (a) or (b), respectively, Neptune is in its position in which it was in JDT = 2451600.5, and TPs cross their asceding node. The integration terminates at the moment, when the star reaches, again, the heliocentric distance of 10 000 AU or 20 000 AU in the post-perihelion arc of its orbit.

Our set of TPs represents the dynamical properties of the CKBOs in the region of heliocentric distances from 35 to 100 AU. To respect also physical properties of these CKBOs, we assume that each considered TP moreover represents a swarm of real bodies of all potentially observable sizes. Assuming the same size distribution and surface properties (albedo) of all TNOs in the considered region, we can associate the same swarm of size-different particles to each TP. The difference in size corresponds to a difference in the absolute magnitude, $H$, a parameter necessary for the determination of an apparent magnitude, $m$. The latter is one of quantities determining the discovery probability. We derive the distribution of $H$ of the CKBOs in the disc before a potential strong stellar perturbation from the current $H$-distribution of the CKBOs.

For a given effective radius of a CKBO, $R$, its apparent brightness can be calculated as

$$m = m_\odot - 2.5\,log_{10}[A_R\Phi(\alpha')R^2] + 5\,log_{10}(1.496 \times 10^8 rr_g). \qquad (1)$$

In this relation, $m_\odot = -27.1$ is the apparent red magnitude of the Sun, $A_R$ is the geometric red albedo, $\Phi(\alpha')$ is Bowell et al.'s (1989) phase function, and $r_g$ is the geocentric distance of the object. Following Trujillo et al. (2001a), we adopt $A_R = 0.04$ consistent with a dark Centaur-like albedo. Trujillo et al.'s sky survey, considered below, was performed at large heliocentric distances $r$ (beyond Neptune) and in the fields of sky near the opposition, i.e. at $\alpha' = 0$, therefore the phase function $\Phi(0) \doteq 1$ and geocentric distance $r_g \doteq r - 1$.

## 3. The calculation of the discovery probability

In our search for the appropriate perturbing-star parameters and its encounter geometry, we determine a probability of the discovery of considered representative CKBOs in their orbits at the end of the performed numerical integration. When the perturbing star leaves the vicinity of the Solar System, we approximate the orbits of the TPs with the Keplerian cone-section curves. In a sub-

sequent evolution, only a small amount of these orbits can be expected to be changed due to rare strong perturbations by Neptune.

In the following, we consider the survey for the new TNOs by Trujillo et al. (2001a), within which the largest number of TNOs have been discovered till now. According Trujillo et al.'s model of the distribution of TNO radii, the distribution can be described by a power law,

$$n(R)\,dR \propto R^{-\nu}\,dR, \tag{2}$$

where the index $\nu = 4.0$ for the CKBOs. The order of the upper limit of effective radius $R$ is identified with the order of the size of Pluto, i.e. with the value of 1000 km. In computations, the lower limit equal to 10 km is considered. However, the condition $m < m_{lim}$ (see below) obviously eliminates bodies above a much larger size.

Concerning the radial distribution of the planetesimals in the proto-planetary disc, we use Hayashi's (1981) model of the disc, where the surface density of the dust was found to be proportional $\propto r^{-3/2}$. This law fits well the current mass distribution of planets (a recent transparent demonstration of the fit can be found in the paper by Morbidelli and Brown, 2004, Fig. 2 on page 177) and has often be generalized to describe the radial distribution of small bodies in the proto-planetary disc (e.g. Oort, 1950; Bailey, 1983; Bailey et al., 1990; Dones et al., 2004). To respect the proportionality of $r^{-3/2}$, we assume the same number (i.e. 12) of the TPs at a given heliocentric distance, $r$, in the beginning. This implies the surface density of the primordial disc proportional to $r^{-1}$. Then, we assign the weight $w = r^{-1/2}$ to each TP at the distance $r$ to transform our proportionality $r^{-1}$ to the actual behaviour, $r^{-3/2}$, of the radial distribution of TPs.

In a prevailing part of the surveys to detect new TNOs, observers have scanned a narrow belt of sky at the ecliptic, where a great majority of discoveries have been made. Trujillo et al. also discovered 74 of 86 TNOs near the ecliptic. So, we determine the probability of a new TNO discovery primarily for this region.

The north-south extent of the sky field of the used detector was $\approx 0.5$ deg, its field area was $S_1 = 0.330$ deg$^2$, whereby the total area of $S_{tot} = 37.2$ deg$^2$ of ecliptic fields were scanned. Therefore, an object in the angular distance up to $\varphi \approx \pm 0.25$ deg from the ecliptic could be detected. (We consider the angle $\varphi$ as approximate because the field of the detector was aligned to the equator, while we speak about an alignment to the ecliptic. This difference is, however, not important in statistical considerations.) For the object at the heliocentric distance $r$, the angular distance $\varphi$ corresponds to the rectangular $z$-coordinate, where

$$z = r\,sin(\omega + f)\,sin\,i \tag{3}$$

and, at the same time,

$$z = r_g\,sin\,\varphi. \tag{4}$$

In these relations, $\omega$ is the argument of perihelion, $f$ is the true anomaly, $i$ is the inclination of orbital plane to the ecliptic, and $r_g$ is the geocentric distance of the object ($r_g \doteq r - 1$). The object spends time $\Delta t$ within the angular distance $\pm\varphi$ from the ecliptic. This happens twice, at both ascending and descending nodes of orbit. First time, the values of true anomaly $f_{a1}$ and $f_{a2}$ corresponding to $-\varphi$ and $+\varphi$, respectively, are

$$f_{a1} = -arctg\left(\frac{sin\,\varphi}{\sqrt{r^2 sin^2 i/(r-1)^2 - sin^2\varphi}}\right) - \omega, \tag{5}$$

$$f_{a2} = arctg\left(\frac{sin\,\varphi}{\sqrt{r^2 sin^2 i/(r-1)^2 - sin^2\varphi}}\right) + 180° - \omega. \tag{6}$$

Second time, these values are

$$f_{b1} = -arctg\left(\frac{sin\,\varphi}{\sqrt{r^2 sin^2 i/(r-1)^2 - sin^2\varphi}}\right) + 180° - \omega, \tag{7}$$

$$f_{b2} = arctg\left(\frac{sin\,\varphi}{\sqrt{r^2 sin^2 i/(r-1)^2 - sin^2\varphi}}\right) - \omega. \tag{8}$$

These relations are valid for $sin^2 i > [(r-1)/r]^2 sin^2\varphi$. If this condition is not satisfied, then the entire orbit is situated within $\pm\varphi$ from the ecliptic and $f_{a1} = f_{b1} = 0°$, $f_{a2} = f_{b2} = 180°$.

Now, we can calculate the exact values $r_{a1}$, $r_{a2}$, $r_{b1}$, and $r_{b2}$, respectively, of corresponding distances by the well-known relation

$$r = \frac{q(1+e)}{1 + e\cos f} \quad , \tag{9}$$

where $q$ and $e$ are the perihelion distance and eccentricity of the object's orbit. Subsequently, the corresponding eccentric and mean anomalies as well as the time intervals $\Delta t_1$ and $\Delta t_2$ can be calculated with the help of classical formulas of the Kepler two-body problem. The partial probability that the object is situated just within $\pm\varphi$ from the ecliptic at the moment of a specific observation is given by the ratio $\Delta t/P$, where $P$ is the orbital period of the object.

The partial probability that the object is projected just to the angular area $S_1$ covered by the used detector in a single exposure is $S_1/S_b$ and partial probability of such a projection in whatever of $n_{exp}$ performed exposures is $n_{exp}S_1/S_b = S_{tot}/S_b$. Here, $S_b$ is the total area of the ecliptical belt of width $\pm\varphi$, i.e. $S_b = 2\varphi.360°$.

Of course, an object can be discovered at the heliocentric distance $r$ within a sky survey, only if its apparent brightness $m$ is higher than the limiting magnitude of the survey, $m_{lim}$. The limiting red magnitude of the considered survey

performed by Trujillo et al. (2001a) was 23.7. The apparent magnitude in $r$ can be calculated from relation (1).

Finally, the relative probability of the discovery of a TNO, having the radius between the values $R$ and $R+dR$ and being situated in the heliocentric distance between $r$ and $r + dr$, is

$$p(r) = (\Delta t/P)(S_{tot}/S_b)wn \qquad \text{for} \ \ m \leq m_{lim},$$
$$p(r) = 0 \qquad \text{for} \ \ m > m_{lim}, \qquad (10)$$

where $n = n(R)$ can be computed from distribution (2) with an arbitrary constant of proportionality.

Summing the partial probabilities through the entire possible intervals of $R$ and $r$, i.e. $R \in< 10\,\text{km}, 1000\,\text{km}>$ with step $1\,\text{km}$ and $r \in< 35\,\text{AU}, 100\,\text{AU}>$ with step $0.5\,\text{AU}$, we can calculate the relative discovery probability for every theoretical object in its final orbit, which is found within our numerical integration. Then, we can construct the distribution of the relative discovery probability and reveal the perturbing star parameters and encounter geometry at which an abrupt drop of the probability at $50\,\text{AU}$ eventually appears.

## 4. Results

We can expect that no CKBO can be discovered beyond the border of $50\,\text{AU}$, if the corresponding discovery probability is lower than 0.5. If $N_{found}$ CKBOs are discovered at the distance $r < 50\,\text{AU}$ within a survey, then the truncation at $50\,\text{AU}$, by the perturbing star, can be confirmed finding the ratio of the relative discovery probabilities for the region $r < 50\,\text{AU}$ and $r > 50\,\text{AU}$, $\rho$, larger than $0.5N_{min}$, where $N_{min}$ is the minimum of $N_{found}$ allowed by a statistical fluctuation.

Within the considered sky survey, Trujillo et al. (2001a) discovered 74 TNOs in $37.2\,\text{deg}^2$ of ecliptic fields. Among these 74 objects, 53 are CKBOs and 7 TNOs, which have been lost and their orbit were not determined. Assuming the proportionality that 53/74 of discovered TNOs are likely CKBOs, the total number of the CKBOs discovered in ecliptic fields is $N_{found} = 53 + (53/74).7 \doteq 58$.

The probability to discover a KBO in a single field of sky, imaged by a few CCD exposures, is very low. A lot of exposures have to been taken to discover an object. This implies that the Poisson statistics can be applied, when one wants to evaluate an uncertainty of the number of discoveries. It yields that $58^{+7}_{-8}$ or $58^{+12}_{-18}$ CKBOs was discovered within Trujillo et al.'s survey evaluating the standard deviation of $1\sigma$ (68.27% confidence interval) or $3\sigma$ (99.73% confidence interval), respectively. Taking into account the 99.73% confidence level, $N_{min} = 58 - 18 = 40$. This figure implies $\rho < 20$ to reject stellar perturbations as the cause of the classical Kuiper-belt edge at $50\,\text{AU}$ on the mentioned confidence level. For the non-perturbed proto-planetary disc, the ratio equals: $\rho = 6.0$.
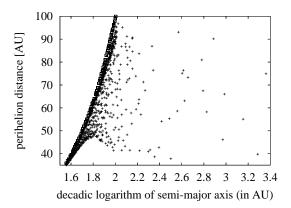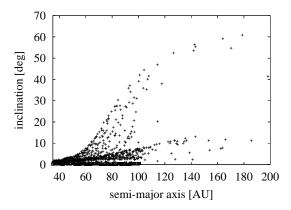
**Figure 1.** The distribution of the test particles, representing the outer edge of the proto-planetary disc, in the log $a-q$ (decadic logarithm of semi-major axis − perihelion distance) space. The open squares illustrate the distribution immediately after the formation of the disc, while the crosses show the distribution after the perturbative stellar passage. The mass of the perturbing star is $0.5\,\mathrm{M_\odot}$, its perihelion distance equals $100\,\mathrm{AU}$, encounter velocity at infinity is $5\,\mathrm{km\,s^{-1}}$, and both argument of perihelion and inclination of the stellar orbit equal $165°$ in this case.



**Figure 2.** The distribution of the test particles, representing the outer edge of the proto-planetary disc, in the $a-i$ (semi-major axis − inclination) space. Few particles on the orbits with $a$ of several thousand AUs are not displayed. The distribution is demonstrated for the same case of the perturbative passage as in Fig. 1. And the symbols with the same meaning are used, too.

**Table 1.** The maximum ratio of the discovery probabilities of TNOs in the regions of heliocentric distance $r < 50$ AU and $r > 50$ AU after the studied stellar perturbation of their original orbits. For each combination of the mass of perturbing star, $M_*$, its perihelion distance, $q_*$, and relative encounter velocity, $v_\infty$, we consider a spectrum of stellar orbital geometries characterized with various arguments of perihelion and inclinations. In the table, the maximum ratio for the entire spectrum is given. For the non-perturbed proto-planetary disc, the ratio would be 6.0. The truncation of the Kuiper belt by a passing star could be explained with the ratio greater than 20 ($3\sigma$ uncertainty level) or, rather, greater than 25 ($1\sigma$ uncertainty level).

| $q_*$ [AU] | $v_\infty$ [km s$^{-1}$] | $M_* = 0.10$, [M$_\odot$] | 0.20, [M$_\odot$] | 0.30, [M$_\odot$] | 0.40, [M$_\odot$] | 0.50 [M$_\odot$] |
|---|---|---|---|---|---|---|
| 70 | 5 | 16.5 | 18.1 | 19.2 | 19.9 | 19.1 |
| | 10 | 13.8 | 13.7 | 12.2 | 14.0 | 14.3 |
| | 15 | 10.5 | 11.7 | 12.4 | 11.8 | 11.1 |
| 100 | 5 | 12.9 | 17.6 | 17.3 | 18.8 | 21.1 |
| | 10 | 11.4 | 17.8 | 18.0 | 18.6 | 18.3 |
| | 15 | 9.4 | 13.6 | 13.1 | 13.3 | 14.0 |
| 200 | 5 | 7.2 | 11.6 | 14.5 | 15.6 | 17.2 |
| | 10 | 6.5 | 9.1 | 12.3 | 15.9 | 14.5 |
| | 15 | 6.1 | 7.4 | 9.3 | 10.7 | 11.2 |
| $q_*$ [AU] | $v_\infty$ [km s$^{-1}$] | $M_* = 0.25$, [M$_\odot$] | 0.50, [M$_\odot$] | 0.75, [M$_\odot$] | 1.00, [M$_\odot$] | 1.25 [M$_\odot$] |
| 500 | 5 | 4.6 | 6.1 | 7.4 | 8.9 | 9.3 |
| | 10 | 4.8 | 5.4 | 6.2 | 6.8 | 7.6 |
| | 15 | 5.3 | 5.5 | 6.1 | 6.9 | 7.1 |
| 1000 | 5 | 4.1 | 4.4 | 4.7 | 5.2 | 5.6 |
| | 10 | 4.6 | 4.6 | 4.6 | 4.7 | 4.9 |
| | 15 | 5.2 | 5.1 | 5.1 | 5.1 | 5.1 |
| 1500 | 5 | 4.2 | 4.3 | 4.5 | 4.6 | 4.8 |
| | 10 | 4.8 | 4.9 | 5.0 | 5.1 | 5.1 |
| | 15 | 5.2 | 5.2 | 5.2 | 5.2 | 5.2 |

We determine $\rho$ for every considered combination of $M_*$, $q_*$, $v_\infty$, $\omega_*$, and $i_*$ (Sect. 2). The maximum $\rho$ of all possible pairs $\omega_*$ and $i_*$ for a given combination of $M_*$, $q_*$, and $v_\infty$ is given in Table 1. Only one value of $\rho$ slightly exceeds the critical $3\sigma$ limit of 20. It is the value of $\rho$ for the combination $M_* = 0.5\,$M$_\odot$, $q_* = 100\,$AU, $v_\infty = 5\,$km s$^{-1}$, $\omega_* = 165°$, and $i_* = 165°$, which we, hereinafter, refer to as the "maximum-$\rho$ combination". For this combination, the dependences $q = q(\log a)$, $i = i(a)$, $i = i(q)$, and $e = e(q)$ of considered TPs after their orbits were perturbed, are illustrated in Figs. 1−4. In Figs. 2, 3, and 4, we can see an excitation of the inclination and eccentricity, respectively, which resembles the
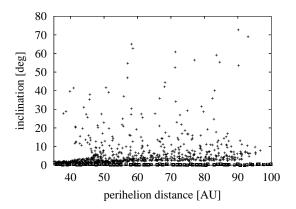
**Figure 3.** The distribution of the test particles, representing the outer edge of the proto-planetary disc, in the $q - i$ (perihelion distance − inclination) space. The distribution is demonstrated for the same case of the perturbative passage as in Fig. 1. And the symbols with the same meaning are used, too.

excitation observed in the classical Kuiper belt. The values of $\rho$ for the other combinations of $M_*$, $q_*$, and $v_\infty$ are smaller than 20 (Table 1), though some of them approach the critical value. No found value of $\rho$ approaches the critical value of 25, which corresponds to the 68.27% confidence level.

Looking at Table 2 giving the amplitude of the velocity-vector change of the Sun, when it is perturbed by the given, nearly passing star, we must, however, state that even the above single positive finding, the maximum-$\rho$ combination, has to be discarded as a proof of the belt truncation, because the velocity change of the Sun would have been so large that the Oort cloud would have been stripped and no dynamically new comets could be observed. Specifically, the amplitude of the velocity change is about $1.6\,\mathrm{km\,s^{-1}}$, while the maximum at which the comet cloud can persist is estimated to be about $0.2\,\mathrm{km\,s^{-1}}$ (Levison et al., 2004).

This criterion discards not only the maximum-$\rho$ combination of stellar orbital parameters, but all the combinations with high $\rho$, approaching the critical value. The values given in Table 2 imply that only relatively larger perihelion distances and lower masses of the perturbing stars do not strip the comet cloud.

As mentioned in Sect. 2, we integrated the orbits of TPs during the passage of the considered star within a sphere of a certain radius. This period, equal to 18 568 years for the maximum-$\rho$ combination of perturbing-star parameters, turns out to be too short for a complete sweeping up the bodies by Neptune from an adjacent region. When we continue to integrate the orbits of TPs for the maximum-$\rho$ combination during another four star-passage periods (92 839 years in total), Neptune changes the orbits of further TPs and $\rho$ decreases from 21.1 to 18.8, i.e. below the critical value of 20. The necessity of taking into account
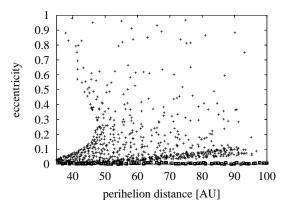
**Figure 4.** The distribution of the test particles, representing the outer edge of the proto-planetary disc, in the $q - e$ (perihelion distance − eccentricity) space. The distribution is demonstrated for the same case of the perturbative passage as in Fig. 1. And the symbols with the same meaning are used, too.

Neptune's perturbation can also be demonstrated by the fact that $\rho$ is larger than 21.1 when this perturbation is omitted. Specifically, $\rho = 21.8$ in the case of the maximum-$\rho$ combination.

## 5. Conclusion

A stellar perturbation tends to increase the number density of the classical CK-BOs inside 50 AU at some encounter parameters. However, Neptune simultaneously reduces again this number density. The ratio of the discovery probabilities of CKBOs within 50 AU and beyond this distance slightly exceeds or closely approaches a critical ratio for some combinations of the encounter velocity, orbital geometry, and mass of the perturbing star. Nevertheless, the truncation of the belt at 50 AU cannot be explained by any stellar passage characterized by these incriminate combinations, because the simultaneous change of the velocity of Sun turns out to be so large that the Oort cloud would have been stripped and no dynamically new comets could be observed.

The negative statement about the truncation by a stellar passage is also supported by a very low probability of an occurrence of the passage, close enough to be efficient, during the age of the Solar System. García-Sánchez et al. (2001) determined the relations giving the frequencies of the passages of stars of various spectral types through a sphere of radius $r$. The relations were determined on the basis of data obtained by the HIPPARCOS satellite correcting them for the observational incompleteness. The frequencies calculated using these relations are consistent with the results by other authors. For example, Chujkova et al. (1999), inspecting the HIPPARCOS data, noticed two passages during $\pm 1\,\mathrm{Myr}$

**Table 2.** The amplitude of the velocity-vector change of the Sun (in $\mathrm{km\,s^{-1}}$), when it is perturbed by a nearly passing star with mass $M_*$ and perihelion distance (the minimum star-Sun distance) $q_*$. The velocity of the star relative to the Sun at a very large (infinite) distance is $v_\infty$.

| $q_*$ [AU] | $v_\infty$ [$\mathrm{km\,s^{-1}}$] | $M_* = 0.10$, [$\mathrm{M_\odot}$] | 0.20, [$\mathrm{M_\odot}$] | 0.30, [$\mathrm{M_\odot}$] | 0.40, [$\mathrm{M_\odot}$] | 0.50 [$\mathrm{M_\odot}$] |
|---|---|---|---|---|---|---|
| 70 | 5 | 0.33 | 0.70 | 1.09 | 1.51 | 1.95 |
| | 10 | 0.24 | 0.52 | 0.84 | 1.19 | 1.58 |
| | 15 | 0.17 | 0.38 | 0.61 | 0.87 | 1.16 |
| 100 | 5 | 0.27 | 0.57 | 0.90 | 1.26 | 1.63 |
| | 10 | 0.18 | 0.38 | 0.62 | 0.88 | 1.17 |
| | 15 | 0.12 | 0.27 | 0.44 | 0.63 | 0.84 |
| 200 | 5 | 0.16 | 0.35 | 0.56 | 0.79 | 1.03 |
| | 10 | 0.09 | 0.20 | 0.33 | 0.47 | 0.62 |
| | 15 | 0.06 | 0.14 | 0.23 | 0.32 | 0.43 |
| $q_*$ [AU] | $v_\infty$ [$\mathrm{km\,s^{-1}}$] | $M_* = 0.25$, [$\mathrm{M_\odot}$] | 0.50, [$\mathrm{M_\odot}$] | 0.75, [$\mathrm{M_\odot}$] | 1.00, [$\mathrm{M_\odot}$] | 1.25 [$\mathrm{M_\odot}$] |
| 500 | 5 | 0.20 | 0.48 | 0.82 | 1.23 | 1.70 |
| | 10 | 0.11 | 0.26 | 0.45 | 0.68 | 0.96 |
| | 15 | 0.07 | 0.18 | 0.31 | 0.47 | 0.65 |
| 1000 | 5 | 0.11 | 0.25 | 0.44 | 0.66 | 0.92 |
| | 10 | 0.05 | 0.13 | 0.23 | 0.35 | 0.49 |
| | 15 | 0.04 | 0.09 | 0.15 | 0.23 | 0.33 |
| 1500 | 5 | 0.07 | 0.17 | 0.30 | 0.45 | 0.63 |
| | 10 | 0.04 | 0.09 | 0.15 | 0.23 | 0.33 |
| | 15 | 0.02 | 0.06 | 0.10 | 0.16 | 0.22 |

of stars with a mass of the solar order within about $0.5\,\mathrm{pc}$. Summing through all spectral types having mass $M_* \geq 0.5\,\mathrm{M_\odot}$, the corresponsding probability by García-Sánchez et al.'s relations is 2.06. When we use these relations to find a probability of stellar passage during the age of the Solar System, regardless of a spectral type, even within the largest distances used in cases (a) and (b) (see Sect. 2), i.e. $200\,\mathrm{AU}$ and $1\,500\,\mathrm{AU}$, we obtain probabilities 0.044 and 2.5, respectively. Corresponding values for more efficient stellar perturbers with the mass $M_* \geq 0.5\,\mathrm{M_\odot}$ are 0.017 and 0.98, respectively. Since only in the case (a) we can obtain an interesting result, only the value of 0.017 is actual. It implies that even a single passage during the entire age of the Solar System is improbable.

In conclusion, no stellar encounter with a relative velocity comparable or larger than about $5\,\mathrm{km\,s^{-1}}$ could cause the truncation of the Kuiper belt after the epoch, when the macroscopic bodies in the belt and a significant fraction of the Oort cloud were formed.

# References

Allen, R.L., Bernstein, G.M., Malhotra, R.: 2001, *Astrophys. J.* **549**, L241

Allen, R.L., Bernstein, G.M., Malhotra, R.: 2002, *Astron. J.* **124**, 2949

Astronomical Almanac for the Year 2000: 1999, Nautical Almanac Office US Naval Obs./Her Majesty's Nautical Almanac Office Rutherford Appleton Lab., Washington/London, p. E3

Bailey, M.E.: 1983, *Mon. Not. R. Astron. Soc.* **204**, 603

Bailey, M.E., Clube, S.V.M., Napier, W.M.: 1990, *The Origin of Comets*, Pergamon, Oxford

Bowell, E., Hapke, B., Domingue, D., Lumme, K., Peltoniemi, J., Harris, A.: 1989, in *Asteroids II*, ed.: R. Binzel, T. Gehrels, and M. Matthews, Univ. Arizona Press, Tucson, 524

Chiang, E.I., Brown, M.E.: 1999, *Astron. J.* **118**, 1411

Chujkova, N.A., Nagoga, M.A., Maximova, T.G.: 1999, in *Evolution and Source Regions of Asteroids and Comets, proc. IAU Coll. No. 173*, ed.: J. Svoreň, E. M. Pittich, and H. Rickman, Astron. Inst., Slovak Acad. Sci., Tatranská Lomnica, 279

Dones, L., Weissman, P.R., Levison, H.F., Duncan, M.J.: 2004, in *Comets II*, ed.: M. C. Festou, H. U. Keller, and H. A. Weaver, Univ. Arizona Press, Arizona, 153

García-Sánchez, J., Weissman, P.R., Preston, R.A., Jones, D.L., Lestrade, J.-F., Latham, D.W., Stefanik, R.P., Paredes, J.M.: 2001, *Astron. Astrophys.* **379**, 634

Gladman, B., Kavelaars, J.J., Petit, J.-M., Morbidelli, A., Holman, M.J., Loredo, T.: 2001, *Astron. J.* **122**, 1051

Hayashi, C.: 1981, *Prog. Theor. Phys. Suppl.* **70**, 35

Ida, S., Larwood, J., Burkert, A.: 2000, *Astrophys. J.* **528**, 351

Jewitt, D., Luu, J., Trujillo, C.: 1998, *Astron. J.* **115**, 2125

Kobayashi, H., Ida, S.: 2001, *Icarus* **153**, 416

Levison, H.F., Duncan, M.J.: 1994, *Icarus* **108**, 18

Levison, H.F., Morbidelli, A., Dones, L.: 2004, *Astron. J.* **128**, 2553

Malhotra, R.: 2001, *Lunar and Planet. Sci.* **XXXII**, 1204

Melita, M.D., Larwood, J.D., Williams, I.P.: 2005, *Icarus* **173**, 559

Morbidelli, A., Brown, M.E.: 2004, in *Comets II*, ed.: M. C. Festou, H. U. Keller, and H. A. Weaver, Univ. Arizona Press, Arizona, 175

Oort, J.H.: 1950, *Bull. Astron. Inst. Netherlands* **11**, 91

Trujillo, C.A., Brown, M.E.: 2001, *Astron. J.* **554**, L95

Trujillo, C.A., Jewitt, D.C., Luu, J.X.: 2001a, *Astron. J.* **122**, 457

Trujillo, C.A., Luu, J.X., Bosh, A.S., Elliot, J.L.: 2001b, *Astron. J.* **122**, 2740